arXiv:0803.2405v2 [cond-mat.supr-con] 19 Mar 2008

Unconventional pairing symmetry in iron-based layered superconductor $LaO_{0.9}F_{0.1-\delta}FeAs$ revealed by point-contact spectroscopy measurements

Lei Shan*, Yonglei Wang, Xiyu Zhu, Gang Mu, Lei Fang, and Hai-Hu Wen*
National Laboratory for Superconductivity, Institute of Physics & Beijing National Laboratory for Condensed Matter Physics, Chinese Academy of Sciences, P.O. Box 603, Beijing 100080, China
(Dated: April 14, 2019)

Superconducting state has lower energy compared with its normal counterpart due to the condensation of paired electrons below T_c. For the electrons of each pair, there is a specific symmetry characterized by the angular momentum number l. For example, the cuprate superconductors are categorized by a d-wave symmetry with $l = 2$ [1], while many conventional superconductors have an s-wave symmetry with $l = 0$. To carry out the pairing symmetry is the first step to resolve the mechanism of a new superconductor. Recently, superconductivity at 26 K [2] was discovered in $LaO_{1-x}F_xFeAs$ (x=0.05-0.12). Here, for the first time, we report point-contact spectroscopy data for junctions between a normal metal and the superconductor $LaO_{0.9}F_{0.1-\delta}FeAs$ (F-LaOFeAs). A zero-bias conductance peak was observed and its shape and magnitude suggests the presence of Andreev bound states at the surface of F-LaOFeAs, which gives a strong evidence of an unconventional pairing symmetry with a nodal gap function. By fitting the spectra to theoretical models for a p-wave or d-wave gap, we obtained the maximum gap value $\Delta_0 \approx 3.9 \pm 0.7$meV.

Copper-based layered superconductors have attracted extensive attention due to their high superconducting transition temperature (T_c) and the underlying rich physics of strong electron correlation. Up to now, however, the mechanism of high temperature superconductivity is still not settled down. In order to open a new path to clarify this issue, much efforts have been devoted to seeking new transition-metal-based superconductors other than cuprates. The exciting discovery of superconductivity in $La[O_{1-x}F_x]FeAs$ with T_c as high as 26K [2] provides a new chance to understand the high-T_c superconductivity and the interplay between magnetism and superconductivity in transition-metal-based superconductors. Interestingly, a nonlinear magnetic field dependence of the low-temperature electronic specific heat coefficient ($\gamma(H)$) has been found in F-LaOFeAs, which is consistent with the prediction for a nodal superconductor such as cuprate superconductors [3]. However, the possibility of novel pairing symmetry in this new superconductor needs to be verified by more experiments especially by phase-related measurements. Point-contact spectroscopy measurements can detect the surface Andreev bound states of a nodal superconductor [4, 5] and thus provides an effective way to determine the pairing symmetry of a new superconductor.

Figure 1a shows the temperature dependence of the resistivity of the sample at 0T and 9T. The onset transition temperature for $H = 0T$ is about 28 K. Since a majority of the sample is superconducting [3], it is feasible to build a point-contact junction between a sharp normal-metal tip and the polished sample's surface. As shown in Fig. 1b and Fig. 3a (raw data) and Fig. 4d (normalized spectra), most of the measured spectra have a distinct zero-bias conductance peak (ZBCP) though the magnitude and shape of the peak varies from one position to another on the sample surface (a featureless spectrum was also observed occasionally at some locations which comes from the non-superconducting region of the sample). This ZBCP is not expected from the s-wave superconductors [6], however, it can be reasonably associated to the surface Andreev bound states and is one of the unique features of a d-wave superconductor [7] (described in METHODS section) and has been demonstrated in the cuprate superconductors such as YBCO and LSCO [4]. The curves calculated for a d-wave superconductor using the extended BTK model (described in METHODS section) are presented in Fig. 1c. A ZBCP can be clearly seen in all curves for different tunneling angle (α) and barrier strength (Z) though its shape and magnitude varies from one to another, which is qualitatively consistent with the measured spectra in this work.

It is necessary to consider other possible origins of the ZBCP observed here before it can be ascribed to the surface Andreev bound states of a nodal superconductor. First, it has been demonstrated that a ZBCP will show up if inter-grain Josephson-coupling effect is in series with the point contact [8], or if the role of critical current becomes dominant due to significant dissipation at the point-contact microconstriction [9]. However, these conjectures are inconsistent with our observations because we can not detect other expected characteristics in these conjectures, namely, two sharp dips in the conductance should exist besides the central ZBCP and the junction resistance should change at the corresponding bias voltage and/or current. Another mechanism for the ZBCP is related to magnetic and Kondo scattering coming from the magnetic impurities in or near the barrier [10]. However, a ZBCP due to magnetic impurities should be uncorrelated with the occurrence of superconductivity. In contrast, as shown in Fig. 2, both the magnitude and the

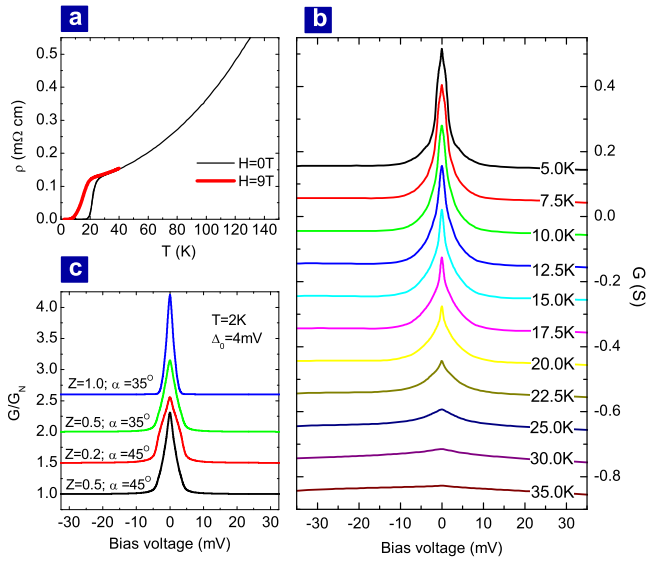

FIG. 1: **ZBCP observed in F-LaOFeAs. a,** Temperature dependence of the resistivity of F-LaOFeAs measured at 0T and 9T. **b,** Conductance-voltage $(G-V)$ characteristics at various temperatures up to above T_c for $H = 0T$. All the curves except the top one are offset downwards for clarity. **c,** Calculated spectra for a nodal superconductor according to the extended BTK model described in METHODS. All the curves except the lowest one are offset upwards for clarity.

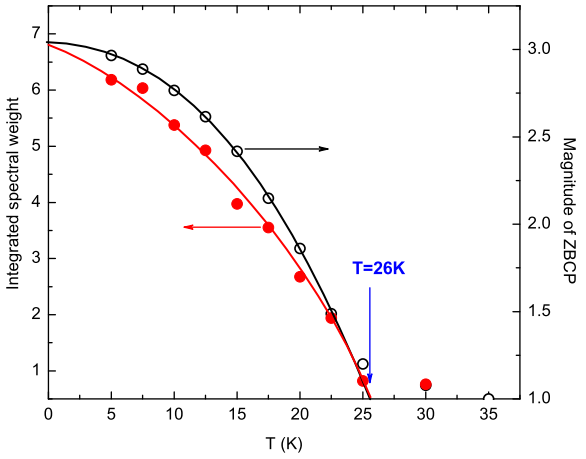

FIG. 2: **Evolution of the characteristics of ZBCP with increasing temperature.** Temperature dependence of the magnitude of ZBCP and the integrated spectral weight. Both parameters are obtained from the spectra shown in Fig. 1b after normalization by the data of 35K.

integrated spectral weight of ZBCP in the present experiment were found to build up rapidly just below 26K, very close to the bulk T_c. In addition, the magnitude of the ZBCP caused by magnetic impurities should depend on temperature logarithmically [10], which is also inconsistent with our data. All these considerations suggest that the ZBCP observed here is most possibly related to

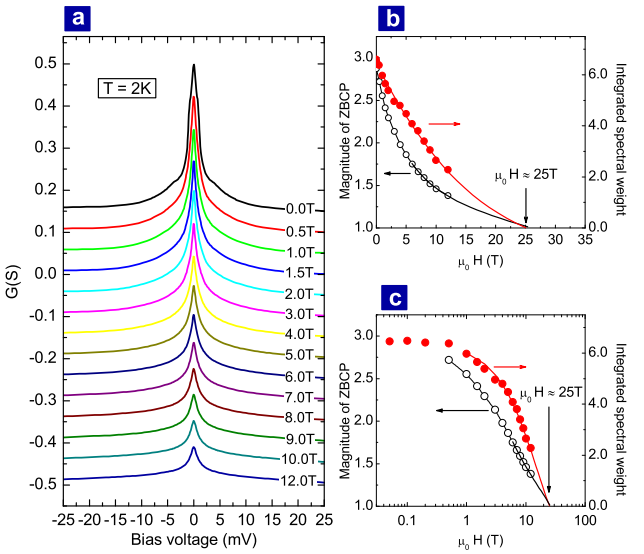

FIG. 3: **Evolution of ZBCP with increasing field. a,** $G-V$ curves measured in various magnetic fields for $T = 2K$. All the curves except the top one are offset downwards for clarity. **b,** Field dependence of the magnitude of ZBCP and the integrated spectral weight. Both parameters are obtained from the spectra shown in **a** after normalization by the data of 35K. **c,** Same data as that in **b** while the horizontal axis is in logarithmic scale.

some type of nodal gap function of the F-LaOFeAs.

Figure 3a shows the evolution of the ZBCP with increasing field from 0 to 12T at a fixed temperature of 2K. ZBCP is suppressed continuously and survives up to the highest field in our measurements. We present in Fig. 3b both the height and integrated spectral weight of the ZBCP. The same data are re-plotted in Fig. 3c while the horizontal axis is in logarithmic scale. By extrapolating these two parameters to zero independently, we can obtain consistently the local upper critical field (H_{c2}) of 25T from both Figs. 3b and 3c. This value is much smaller than $H_{c2} > 50T$ estimated from resistivity measurements [11, 12]. As mentioned in Ref.[11], the upper critical field determined from resistivity reflects mainly the situation of $H \parallel a-b$ plane since the Cooper pairs within the grains with this configuration will last to the highest field compared to other grains. Since our point-contact configuration is a local measurement, it may probe the grains with particular orientations, so the determined H_{c2} should locate between $H_{c2}^{ab} \approx 56T$ and $H_{c2}^{c} \approx 6T$ by assuming an anisotropy $\Gamma = H_{c2}^{ab}/H_{c2}^{c} \approx 10$ [11], in agreement with the result in this work.

Dagan *et al.* [13] proposed a simple method to determine the gap value of a nodal superconductor by considering that the peak in the density of states at the gap value should be sensitive to an applied field, while other structures should not be. The method of data analysis consists simply in subtracting conductances measured in

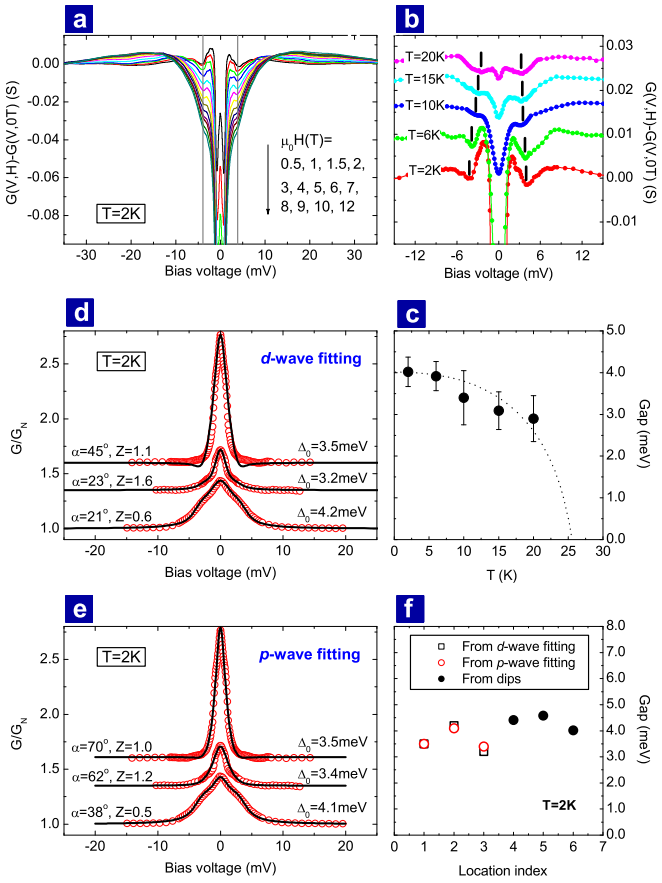

FIG. 4: **Determination of superconducting gap. a,** The conductance of various fields from Fig. 3a after subtraction of the zero-field conductance. **b,** The conductance at low field of 0.5T or 1.0T after subtraction of the zero-field conductance for various temperatures. The positions of the dips in each curve are indicated by short bars. **c,** Maximum superconducting gap determined from the data presented in **b**. **d and e,** Fitting the normalized spectra (open circles) obtained at various locations on the sample surface to the extended BTK model with d-wave and p-wave pairing symmetries, respectively. **f,** Summing up the maximum gap values of various locations on the sample surface determined both by dips and fits.

an applied field, from the zero field conductance. Structures that are not directly related to superconductivity are, in this way, eliminated [13]. When the subtraction procedure is applied to the data of Fig. 3a, as shown in Fig. 4a, very clear dips appear symmetrically around ±4mV and locate at the same bias for fields up to 5T (indicated by two vertical gray lines). This is very similar to the case discussed in Ref.[13] (except that there is a field dependent background here), allowing a precise determination of the gap values. Fig. 4b shows such dip structure for various temperatures and the gap values determined from these dips are presented in Fig. 4c, the decay of the gap value with increasing temperature is obvious.

Figure 4d shows the estimation of the gap values by fitting the normalized spectra (measured at different locations) to the extended BTK model with a $d_{x^2-y^2}$ gap function (described in METHODS). The obtained Δ_0 varies in a range of 1mV, indicating a certain degree of inhomogeneity on the sample surface. It should be mentioned that our data support a nodal gap function of F-LaOFeAs while can not distinguish between d-wave and p-wave. Since the superconducting phase of F-LaOFeAs is located close to the ferromagnetic phase [2], it is possible that spin triplet pairing, such as p-wave pairing symmetry, is favored in this material. In fact, very similar ZBCP was observed in Sr_2RuO_4 single crystal with spin triplet superconductivity [14]. Fig. 4e shows the calculations with a p-wave gap function of $\Delta = \Delta_0 sin\theta$, which is consistent with the experimental data as well as the d-wave fits. In both approaches, the nodal characteristic and the maximum value of the gap function of F-LaOFeAs can be confirmed consistently. In Fig. 4f, we can see that the gap values determined both by fitting procedure and from the dip structure are well consistent with each other, which can be summed up as $\Delta_0 = 3.9 \pm 0.7$meV. This result is in good agreement with $\Delta_0 = 3.4 \pm 0.5$meV from our specific heat measurement [3]. Thus, we can calculate the Bardeen-Cooper-Schrieffer coherence length $\xi_{BCS} = \hbar\nu_F/\pi\Delta_0$ where the in-plane Fermi velocity $\nu_F^{ab} = 1.30 \times 10^7$cm/s [15]. Using $H_{c2}^c \approx 6T$ mentioned above [11], we can calculate the Ginzburg-Landau coherence length $\xi_{GL}^{ab} = \sqrt{\phi_0/2\pi H_{c2}^c}$ with ϕ_0 the flux quantum. The obtained $\xi_{BCS} = 70\mathring{A}$ is in good agreement with the calculated $\xi_{GL}^{ab} = 74\mathring{A}$ within the experimental errors, suggesting that F-LaOFeAs is in the clean limit, which is different from the dirty-limit case of the electron-doped cuprates with similar T_c values [16]. It is also the reason why a clear ZBCP can be observed in this work and the Δ_0 can be derived properly from the specific heat data[3] for F-LaOFeAs.

METHODS:

SAMPLES AND MEASUREMENTS:

The polycrystalline samples of $LaO_{0.9}F_{0.1-\delta}FeAs$ (F-LaOFeAs) were synthesized by using a two-step solid state reaction method. The detailed information about the synthesization is elaborated in a recent paper [3]. The point-contact junctions are prepared by carefully driving the Pt/ Ir alloy or Au tips towards the sample surface which is polished and cleaned beforehand. The tip's preparation and the details of the experimental setup were described elsewhere [8]. Typical four-terminal and lock-in techniques were used to measure the conductance-voltage ($dI/dV - V$ or $G - V$) characteristics. Each measurement is comprised of two successive cycles, to check the absence of heating-hysteresis effects.

THEORETICAL MODELS:

Blonder, Tinkham, and Klapwijk (BTK) [6] have proposed a simple theory for the $G - V$ curves of an s-wave superconductor/normal metal junction separated by a

barrier of arbitrary strength. The barrier strength is parametrized by a dimensionless number Z which describes the crossover from metallic to ideal tunnel junction behavior by $Z = 0$ to $Z = \infty$. It was predicted that no sharp ZBCP could be observed for an s-wave superconductor/normal metal junction with any barrier strength, furthermore, the normalized conductance (G/G_N) at zero bias can not exceed 2, the upper limit of the ideal Andreev reflection. This is obviously not the case of our measurements, in which a distinct ZBCP was observed and its magnitude exceeds 2 occasionally.

Tanaka *et al.* [17, 18, 19] extended the BTK model to deal with the issue of an anisotropic d-wave superconductor. In this case, another parameter α (the angle between the quasiparticle injecting direction and the main crystalline axis) was introduced in addition to the barrier strength Z. Moreover, the isotropic superconducting gap Δ in the s-wave BTK model was replaced by an anisotropic gap with $d_{x^2-y^2}$ symmetry, i.e., $\Delta = \Delta_0 cos(2\theta)$ in which Δ_0 is the maximum gap. It was thus predicted that, for $Z > 0$ the ZBCP is formed for all directions in the $a-b$ plane except when tunneling into the (100) and (010) planes. This ZBCP will be suppressed if the quasiparticle scattering is strong enough [20].

e-mail: shanlei@ssc.iphy.ac.cn (L. Shan), hhwen@aphy.iphy.ac.cn (H. H. Wen)

[1] Tsuei, C. C., & Kirtley, J. R. Pairing symmetry in cuprate superconductors. *Rev. Mod. Phys.* **72**, 969-1016 (2000), and references therein.

[2] Kamihara, Y., Watanabe, T., Hirano, M. & Hosono, H. Iron-based layered superconductor La[$O_{1-x}F_x$]FeAs (x=0.05-0.12) with T_c=26K. *J. Am. Chem. Soc.* **xxx**, xxxx (2008).

[3] Mu, G. *et al.* Nodal gap in Fe-based layered superconductor $LaO_{0.9}F_{0.1-\delta}FeAs$ probed by specific heat measurements. arXiv:0803.0928v1 [cond-mat.supr-con].

[4] Deutscher, G. Andreev-Saint-James reflections: A probe of cuprate superconductors. *Rev. Mod. Phys.* **77**, 109-135 (2005), and references therein.

[5] Löfwander, T., Shumeiko, V. S. & Wendin, G. Andreev bound states in high-T_c superconducting junctions. *Supercond. Sci. Technol.* **14**, R53-R77 (2001).

[6] Blonder, G. E., Tinkham, M. & Klapwijk, T. M. Transition from metallic to tunneling regimes in superconducting microconstrictions: Excess current, charge imbalance, and supercurrent conversion. *Phys. Rev. B* **25**, 4515-4532 (1982).

[7] Hu, C.-R. Midgap surface states as a novel signature for $d_{x^2-y^2}$-wave superconductivity. *Phys. Rev. Lett.* **72**, 1526-1529 (1994).

[8] Shan, L. *et al.* s-wave pairing in $MgCNi_3$ revealed by point contact tunneling. *Phys. Rev. B* **68**, 144510 (2003).

[9] Sheet, G., Mukhopadhyay, S. & Raychaudhuri, P. Role of critical current on the point-contact Andreev reflection spectra between a normal metal and a superconductor. *Phys. Rev. B* **69**, 134507 (2004).

[10] Appelbaum, J. "s-d" exchange model of zero-bias tunneling anomalies. *Phys. Rev. Lett.* **17**, 91-95 (1966).

[11] Zhu, X. *et al.* Upper critical field, Hall effect and magnetoresistance in the iron-based layered superconductor $LaO_{0.9}F_{0.1-\delta}FeAs$. arXiv:0803.1288v1 [cond-mat.supr-con].

[12] Chen, G. F. *et al.* Superconducting properties of Fe-based layered superconductor $LaO_{0.9}F_{0.1-\delta}FeAs$. arXiv:0803.0128v1 [cond-mat.supr-con].

[13] Dagan, Y., Krupke, R. & Deutscher, G. Determination of the superconducting gap in $YBa_2Cu_3O_{7-\delta}$ by tunneling experiments under magnetic fields. *Phys. Rev. B* **62**, 146-149 (2000).

[14] Mao, Z. Q. *et al.* Observation of Andreev surface bound states in the 3-K phase region of Sr_2RuO_4. *Phys. Rev. Lett.* **87**, 037003 (2001).

[15] Singh, D. J. & Du, M. -H. $LaFeAsO_{1-x}F_x$: A low carrier density superconductor near itinerant magnetism. arXiv:0803.0429v1 [cond-mat.supr-con].

[16] Dagan, Y., Beck, R. & Greene, R. L. Dirty superconductivity in the electron-doped cuprate $Pr_{2-x}Ce_xCuO_{4-\delta}$: Tunneling study. *Phys. Rev. Lett.* **99**, 147004 (2007).

[17] Tanaka Y. & Kashiwaya, S. Theory of tunneling spectroscopy of d-wave superconductors. *Phys. Rev. Lett.* **74**, 3451-3454 (1995);

[18] Kashiwaya, S., Tanaka, Y., Koyanagi, M. & Kajimura, K. Theory for tunneling spectroscopy of anisotropic superconductors. *Phys. Rev. B* **53**, 2667-2676 (1996).

[19] Kashiwaya, S. & Tanaka, Y. Tunnelling effects on surface bound states in unconventional superconductors. *Rep. Prog. Phys.* **63**, 1641-1724 (2000).

[20] Aprili, M. *et al.* Tunneling spectroscopy of the quasiparticle Andreev bound state in ion-irradiated $YBa_2Cu_3O_{7-\delta}$/Pb junctions. *Phys. Rev. B* **57**, R8139-R8142 (1998).

Acknowledgments

This work is supported by the Natural Science Foundation of China, the Ministry of Science and Technology of China (973 project No: 2006CB601000, 2006CB921802, 2006CB921300), and Chinese Academy of Sciences (Project ITSNEM).

Competing financial interests

The authors declare no competing financial interests.